Brief Report

Adjuvant oligonucleotide vaccine increases survival of transgenic mice [B6.Cg-Tg (K18-ACE2)2]

Volodymyr V. Oberemok, Kateryna V. Laikova, Kseniya A. Yurchenko, Ilya A. Novikov, Tatyana P. Makalish , Anatolii V. Kubyshkin, Oksana A. Andreeva, Anastasiya I. Bilyk

V.I. Vernadsky Crimean Federal University, Simferopol, Crimea
Correspondence: voloberemok@gmail.com; Tel.: +7(978)8146866

Abstract: The main problem in creating anti-coronavirus vaccines that target mainly proteins of the outer membrane of the virus remains the rapid variability of the RNA genome of the pathogen that encodes these proteins. In addition, the introduction of technologies that can provide affordable and fast production of flexible vaccine formulas that easily adapt to the emergence of new subtypes of SARS-CoV-2 is required. Universal oligonucleotide vaccine can take into account the dynamics of rapid changes in the virus genome, as well as be synthesized on automatic DNA synthesizers in large quantities in a short time. In this brief report, the effectiveness of four phosphorothioate constructs of the La-S-so type oligonucleotide vaccine will be evaluated for the first time on transgenic mice [B6.Cg-Tg (K18-ACE2)2]. In our primary trials, the oligonucleotide vaccine increased the survival rate of animals infected with SARS-CoV-2 and also reduced the destructive effects of the virus on the lung tissue of mice. The obtained results show the perspective of the development of vaccine constructs of the La-S-so type for the prevention of coronavirus infections, including those caused by SARS-CoV-2.

Keywords: oligonucleotide vaccines, SARS-CoV-2, phosphorothioate oligonucleotides, innate immunity, adaptive immunity

1. Introduction

As of March 10, 2023 according to the Johns Hopkins University Coronavirus Resource Center, more than 676 million people had fallen ill, and more than 6.8 million had died, more than 13.3 billion vaccine doses have been administered worldwide [1]. The COVID-19 pandemic is now considered to be over. [2]. However, outbreaks of the disease continue to be recorded throughout the world. [3, 4, 5]. Obviously, the microevolution of SARS-CoV-2 will continue, and new subtypes will arise that can eventually lead to the next pandemic. Due to the lack of specific drugs that can provide reliable protection, vaccines are an effective tool for preventing COVID-19 in this situation. To date, there are three main platforms for vaccines: inactivated [6], adenoviral vectors [7], and mRNA vaccines [8]. However, all three platforms have side effects on human health. For example, the inactivated CoronaVac vaccine causes pain at the injection site, headache, fatigue, muscle and joint pain [9]. The adenovirus vaccine, using VaxZevria as an example, was manifested by frequent systemic reactions in the form of fatigue, myalgia, headache, fever, and atypical thrombosis [10, 11]. Humans have reported glomerulonephritis as one of the most serious side effects following Moderna injection [12]. In addition, all of the listed vaccine platforms do not provide the long operational half-life associated with the rapidly changing SARS-CoV-2 RNA genome. One of the promising ways to create anti-coronavirus vaccines is to use conservative regions of the coronavirus genome to create universal vaccines; however, this issue is still under study. Thus, from the point of view of improving the safety and duration of action of vaccines and the search for new platforms is relevant. Of interest is the postgenomic platform for creating vaccines [13], which is based on the use of nucleotide sequences of RNA viruses as antigens and not just adjuvants [14]. The avalanche accumulation of SARS-CoV-2 genomic sequences contributes to this direction of the search.

 doi:10.20944/preprints202305.1794.v1

In this brief report, for the first time, we will try to answer the question of the viability of the idea of oligonucleotide vaccines using a practical example. For this study, we will use the transgenic mice [B6.Cg-Tg (K18-ACE2)2] and four 'La-S-so' constructs containing an antigen-presenting 'head' with a specific sequence in order to activate adaptive immunity, a tail with CpG islands to activate innate immunity, and 'neck', 'connecting 'head' and 'tail'. In addition, in the article we will consider two routes of administration: subcutaneous and intranasal.

2. Materials and Methods

2.1. Design, synthesis and purification of a La-S-so type oligonucleotide vaccine

We used phosphorothioate oligonucleotide constructs for our experiments:

La-S-so-1

5'-(CCCCCGGGGG)$_{'neck'}$(GCAGAGACAGAAGAAACAGCAAAC)$_{'head'}$(CCCCCGGGGG)$_{'neck'}$(AACGCCAACGCC)$_{'tail'}$-3';

La-S-so-2

5'-(CCCCCGGGGG)$_{'neck'}$(AGGCACAACAACAAGGCCAAAC)$_{'head'}$(CCCCCGGGGG)$_{'neck'}$(AACGCCAACGCC)$_{'tail'}$-3';

La-S-so-3

5'-(CCCCCGGGGG)$_{'neck'}$(AACAAGACAAAAACACCCAAGAAG)$_{'head'}$(CCCCCGGGG)$_{'neck'}$(AACGCCAACGCC)$_{'tail'}$-3';

La-S-so-4

5'-(CCCCCGGGGG)$_{'neck'}$(CACCGAGGCCACGCGGAG)$_{'head'}$(CCCCCGGGGG)$_{'neck'}$(AACGCCAACGCC)$_{'tail'}$-3'.

The vaccine was designed using SARS-CoV-2 genome sequences, the GenBank database was used to search for conserved regions, and the ClustalW 2.0.3 programs were used to align oligonucleotide sequences [15]. In our 'La-S-so' construct, we placed the CpG motifs in the 'tail' region in the 5′-purine-purine-unmethylated deoxycytosine-deoxyguanosine-pyrimidine-pyrimidine-3' position [16]. The 'neck' region of the construct features a double-stranded DNA region stabilized by 30 hydrogen bonds between 10 cytosines and 10 guanines. The double-stranded DNA 'neck' makes it possible to form a loop in the region of the antigen-presenting 'head'. The general look of the La-S-so type vaccine was represented in [17]. Only adenines, cytosines, and guanines are present in the construct, which makes it possible to activate pattern recognition receptors interacting with both 'non-self' DNA and 'non-self' RNA. Since the PS backbone is the basis of the construct, the presence of deoxyribose will be of little importance and everything will depend on the nucleotide sequence of the construct [18]. Also, CpG motifs in nuclease-resistant PS backbones have been found to dramatically enhance B cell stimulatory properties [19, 20].

The developed vaccine was synthesized on the ASM-800 DNA synthesizer (BIOSSET, Russia) using standard phosphoramidite synthesis. The synthesis was carried out in the direction from the 3' to the 5' end. After completion of all cycles of synthesis, the target oligonucleotide is removed from the solid-phase carrier; the removal of the protective groups was carried out overnight at 55°C in a concentrated ammonia solution [21]. Purification of the synthesized vaccine was performed by reverse-phase high-performance liquid chromatography (RP-HPLC) on a Jupiter 5μm C18 300 Å column (4.6 mm × 250 mm) using a preparative HPLC system (Azura P6.1 L, UVD 2.1S detector). Buffers were used for purification: (A) 0.1 M triethylammonium acetate in water, (B) 50% MeCN/buffer A. Gradient 30%.

 doi:10.20944/preprints202305.1794.v1

2.2. Animals and experimental groups

Transgenic mice [B6.Cg-Tg (K18-ACE2)2] (The Jackson Laboratory, USA) at the age of 7 weeks were randomly divided into 4 groups: 1) intact, 2) with SARS modeling without treatment, 3) two intranasal injections of the vaccine with an interval of a week, two weeks before the SARS modeling, 4) subcutaneous administration of the vaccine with an interval of a week, two weeks before the SARS modeling. There were six mice in each group. The animals were kept in specific pathogen free cages inside laminar flow hoods of the 2nd class of protection with free access to water and food.

2.3.Vaccination

The oligonucleotide vaccine was administered intranasally and subcutaneously twice, at weekly intervals, in an amount of 30 μl at a concentration of 1000 ng/μl. Injections were carried out using an insulin syringe, and in the case of intranasal administration, the vaccine was administered intranasally with a pipette dispenser. During intranasal administration, mice were immersed in anesthesia and the vaccine was added to the nasal passages for further reflex inhalation and the vaccine entering the respiratory tract.

2.4. Weighing

The weight of mice was measured every day on an Ad100 scale (Axis, Poland) with a precision of 0.001 g.

2.5. Mice infestation

SARS was modeled by intranasal administration of a suspension of virus particles. Biomaterial from 15 patients (2 μl each) with PCR-confirmed SARS-CoV-2 was mixed with a 0.9% NaCl solution, after which it was injected into mice in an amount of 30 μl of liquid, and thus all animals received relatively equal doses in terms of virulence. When using the Polivir SARS-CoV-2 Express kit (Litekh, Russia), according to the instructions, Cq in these patients was always in the range from 17 to 18 cycles. For RNA isolation, 100 μL of a swab in 0.9% NaCl solution was used, and then 3.5% of the isolated RNA was used for RT-PCR.

2.6. PCR procedure

The infection of mice was confirmed by PCR. A swab for PCR analysis was taken from the oral cavity of mice. The resulting smear was placed in a test tube with a 0.9% NaCl solution. RNA was isolated using the "Polivir SARS-CoV-2 Express" kit (Litekh, Russia) according to the instructions. PCR was performed with a kit for polymerase chain reaction with reverse transcription "Polivir SARS-CoV-2 Express" kit (Litekh, Russia) according to the instructions. The work was carried out on a real-time cycler CFX96 Touch (Bio-Rad, USA).

2.7. Autopsy of model animals

Animals from the intact group and those receiving the vaccine were euthanized by intramuscular injection of chloral hydrate at a dose of 200 mg/kg of live weight, after which they were decapitated.

The autopsy was carried out in several stages: fixation of the limbs of the animal with dissection needles on the dissecting tray with its back down. Next, the skin was captured and lifted with tweezers; a longitudinal incision was made along the white line of the abdomen from the inguinal region to the region of the lower jaw. The abdominal wall must remain intact. The skin was pushed back along the edges of the abdominal wall and fixed.

An incision was made in the abdominal wall from the inguinal region to the midline of the abdomen, and an incision was made in the chest with scissors. After that, the lungs were carefully removed and the target organs were placed in histological cassettes. Organs were stored in 10% buffered formalin for 12 hours to prepare for immunohistochemical analysis.

 doi:10.20944/preprints202305.1794.v1

2.8. Immunohistochemical assay

Dehydration and paraffin impregnation were carried out in a Logos microwave histoprocessor (Milestone, Italy). Tissue blocks were sectioned 4 μm thick and stained with hematoxylin and eosin. Reagents for fixation, dehydration, wiring and staining manufactured by Biovitrum (Russia) were used: formalin 10%, isopropyl alcohol, paraffin, o-xylene, a set of dyes hematoxylin and eosin, recommended for histological studies. Stained sections were scanned on an Aperio CS2 scanner (Leica, USA) for morphometric analysis of changes in the lungs, 10 fields of view in each section were selected in the Aperio ScanScope program, the relative areas occupied by the lumen of the alveoli and bronchi, interalveolar septa, vessels, areas of edema and fibrosis were calculated.

2.9. Statistical data processing

Statistical processing was carried out using the program STATISTICA 10. The normality of the distribution of the trait was determined by the Shapiro-Wilk method. The mean values of indicators, standard deviation, and error of the mean, upper and lower quartiles were calculated. The Kruskal-Wallis method was used to compare scores between groups. Differences were considered significant at $p < 0.05$.

The study was approved by the ethics committee of the Federal State Autonomous Educational Institution of Higher Education V.I. Vernadsky Crimean Federal University. Vernadsky" dated October 01, 2021 protocol No. 25/21 When conducting experimental studies, the principles and provisions of the Guide for the Care and Use of Laboratory Animals (USNIH, No. 85-23), international rules "Guide for the Care and Use of Laboratory Animals" (2009), taking into account the Council of Europe Convention for the Protection of Vertebrate Animals used for Experimental or other Scientific Purposes (Strasbourg, 1986).

3. Results

In the course of the studies, a decrease in the weight of animals of the infected control was found on the 8th day of the experiment compared with individuals from the groups where vaccination was carried out (Figure 1). Weight loss is a nonspecific sign in viral diseases, including COVID-19 [22-25]. It can be concluded that the applied four constructs of the La-S-so type oligonucleotide vaccine were able to save the animals from weight loss, which is consistent with the data of the organometric parameters of the lungs of mice (Table 1).

In groups using the oligonucleotide vaccine, the timing of the onset of the disease did not differ, the manifestation of the disease was pronounced, however, on average, hyperthermia was lower by 1.2°C, and the clinical condition of the animals recovered faster.

On the second day, there was no significant difference in weight between the positive and negative controls, in contrast to the experimental groups, where a significant difference was already observed on the second day of the experiment. On the 4th day, a linear increase in body weight was noted in the positive group and in the experimental groups, where the weight increased every second day, compared with the negative control group, where the weight was in a plateau state throughout the experiment ($p < 0.05$). On the 8th day, the weight of the negative control decreased by 0.89±0.19 g; by the 10th day, the weight of the animals increased by 0.86±0.09 g, which corresponds to the weight of the animals on the 6th day of the disease. This suggests that the administration of the vaccine (intranasal and subcutaneous) prevents weight loss when infected with COVID-19.

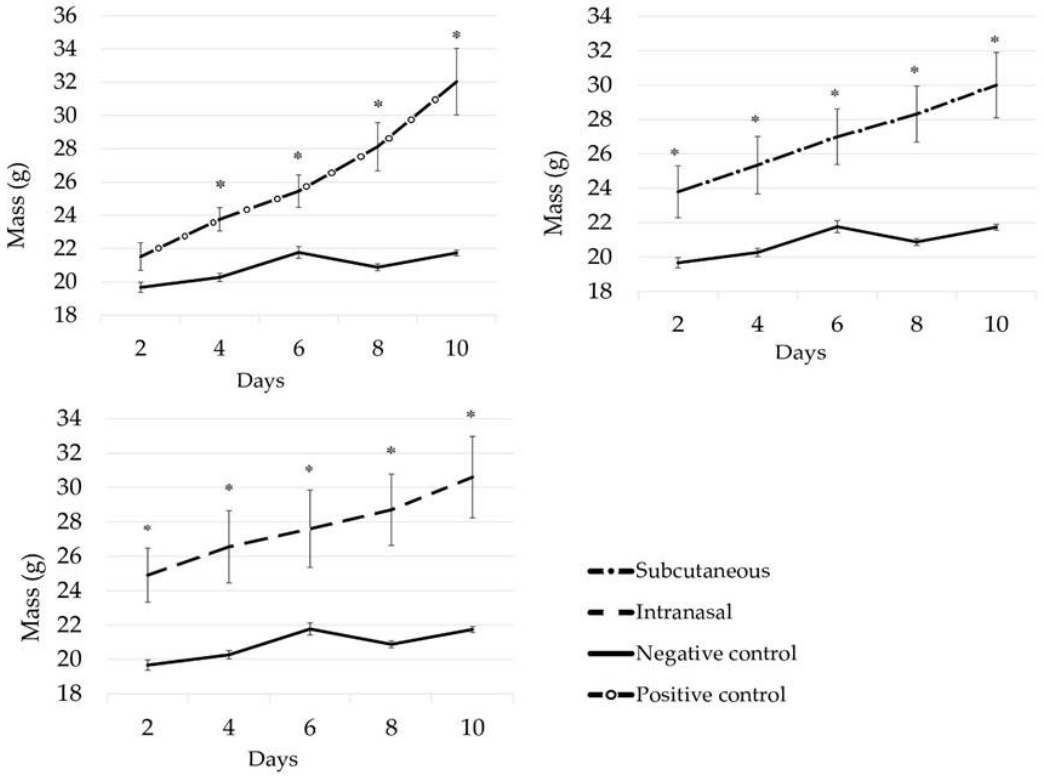

Figure 1. Change in the mass of mice in groups: a) negative and positive controls; b) negative control and subcutaneous administration; c) negative control and intranasal administration. *significant difference compared to the negative control group ($p < 0.05$)

Histochemical studies showed a picture similar to organometric indicators. The analysis of morphometric data showed significant changes in the area of various parts of the lung (Figure 2). The dynamics were revealed in the study of three parameters of tissue sections: areas of edema, vessels, and lumen of the alveoli. Interalveolar and perivascular edema in all groups becomes significant on the 5th day, but decreases on the 10th day and subsides by the 30th day, its area becomes significantly lower relative to the early stages of the disease. Congestion and vascular area are most pronounced in the group with intranasal administration of the vaccine. At the beginning of the disease on the 5th day in all groups, the greatest dilatation of capillaries is observed. On the 10th day in the group without treatment and with treatment, alveolar-hemorrhagic syndrome was noted in about half of the animals. The area of the lumen of the alveoli in animals is significantly reduced due to distlectasis and atelectasis on the 10th day of illness in all groups, except for the group with intranasal administration of the vaccine. It is this indicator that is the key, in our opinion, since it is most pronounced in the group without treatment and is clinically accompanied by lethality, noted only in this group.

In the mice from the group without the use of the vaccine, on the 5th day after infection in the lung parenchyma, significant areas of dyslectasis and atelectasis, thickening of the interalveolar septa, edema and lymphocyte infiltration of the alveoli and bronchi, and desquamation of the epithelium of the bronchioles were detected. By the 10th day, proliferation of type II alveolocytes developed, fibrin clots appeared in the lumen of the vessels, hemorrhages into the lumen of the alveoli, and single hemosiderophages. Between the 10th and 30th days of the disease, all animals from this group died at night, which did not allow the revealed changes in the structure of the lung to be interpreted as associated with the development of SARS, since autolysis additionally destroyed tissues.

 doi:10.20944/preprints202305.1794.v1

Table 1. Organometric parameters of the lungs of mice with simulated SARS in different groups of the experiment

Area % Group		Stroma	Edema	Vessels	Lumen of the alveoli	Fibrosis
Intact (i)		40,0 [34.0;42.0]	0 [0.0;0.0]	12,50 [10.0;14.0]	47,50 [43.0;50.0]	0 [0.0;0.0]
Intranasal vaccine (n)	5 day	30,50+ [27.5;34.0]	7,50+ [50;9.0]	21,50* [14.0;28.5]	37,00 [31.5;44.5}	1,50 [1.0;3.0]
	10 day	40,00□ [37.0;45.0]	5,00 [3.0;7.0]	19,50 [13.0;31.0]	30,50* [25.0;41.0]	1,00 [0.0;1.0]
	30 day	41,50□ [39.0;45.5]	2,00□ [1.0;4.0]	13,50 [9.5;17.0]	42,00 [35.0;45.0]	1,00 [0.0;1.0]
Subcutaneous vaccine(s)	5 day	35,00 [32.0;38.5]	8,00+ [6.0;12.5]	17,00 [12.0;21.5]	39,50 [34.5;42.5]	1,00 [1.0;2.0]
	10 day	45,50 [42.0;48.0]	8,00 [8.30;13.0]	17,50 [17.0;23.0]	25,50* [24.0;29.0]	2,00 [2.0;3.0]
	30 day	39,50 [36.0;47.5]	3,00□ [1.5;4.0]	16,50 [15.5;22.5]	37,50□ [32.5;41.0]	1,00 [1.0;1.0]
Model without treatment (c)	5 day	40,50 [37.5;46.5]	5,00 [4.0;8.5]	15,00 [11.0;27.0]	32,50 [22.0;41.5]	1,00 [0.0;1.5]
	10 day	43,50 [38.0;50.0]	8,00 [5.0;10.0]	25,00 [21.0;28.0]	20,00* [19.0;25.0]	1,50 [1.0;2.0]
	30 day	x	x	x	x	x

Note: differences between groups were determined by comparing many independent samples using the Kruskal-Wallis method and were considered significant at $p < 0.05$; * – differences from the intact group; + - differences from the group without treatment at the corresponding time of the experiment; □ – differences within the group at different periods of the experiment (compared to 5 days); X – for this variant, the study was not carried out due to lack of information.

In mice of the group with subcutaneous application of the vaccine, on the 5th day of the development of the disease, edema of the interalveolar septa, areas of emphysema, extensive areas of lymphoid infiltration, hemorrhages, plethora of large vessels and capillaries were observed. On the 10th day, the area of the lumen of the alveoli decreased due to atelectasis and proliferation of alveolocytes, the vessels remained full-blooded, areas of fibrosis and fibrin fibers appeared in the lumen of the vessels. By the 30th day, the area of the lumen of the alveoli slightly increased due to compensatory emphysema, the state of the parenchyma as a whole remained the same.

The use of intranasal vaccine showed the best effect in assessing the morphology of the lungs of experimental animals. At the initial stages (up to 5 days), the course of the disease turned out to be more acute than in other groups and was accompanied by significant edema in the interalveolar septa and paravasal region, lymphoid infiltration, and areas of atelectasis. On the 10th day, the edema became less noticeable, but a focal complete or partial collapse of the alveoli was observed. The vessels still remained full-blooded, single hemorrhages were revealed. By the 30th day, no edema was detected, however, the interalveolar septa remained thickened due to lymphoid infiltration and proliferation of lining cells.

 doi:10.20944/preprints202305.1794.v1

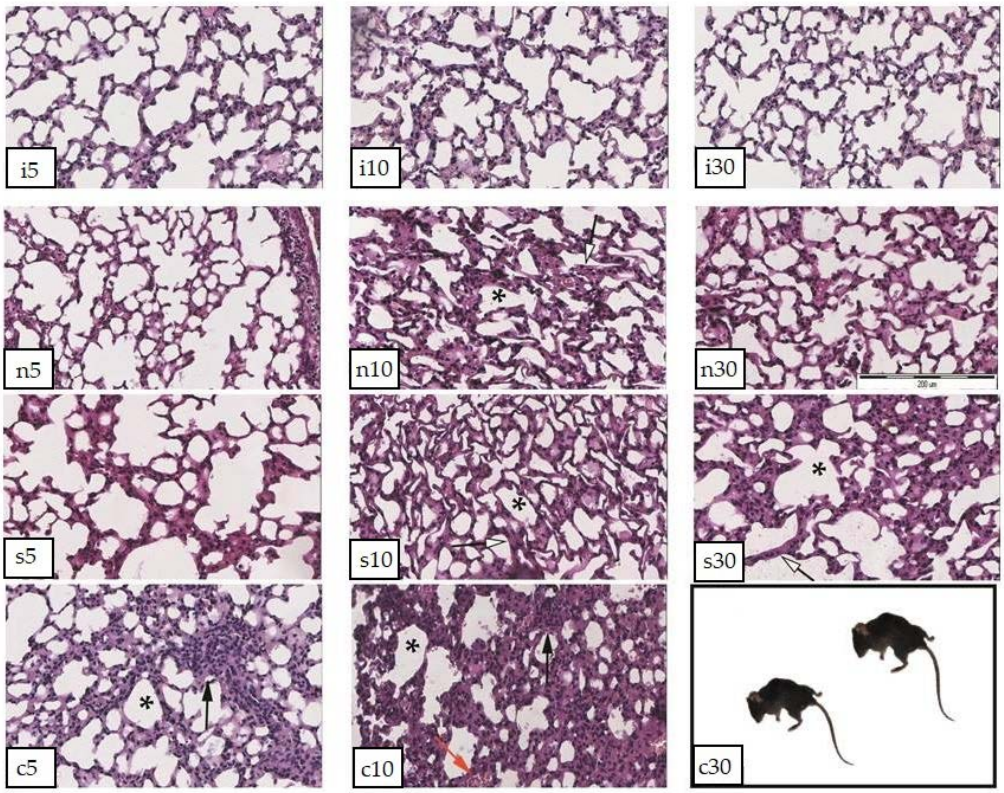

Figure 2. Paraffin sections of the lungs of SARS model mice (except 1A). Stained with hematoxylin and eosin. SW. 20x. 1 A(i) - intact animals, 2 A - SARS model 5 days, 3 A - SARS model 10 days, 1 B (n) - group with intranasal administration of the vaccine, 5 days after infection, 2 B - group with intranasal administration of the vaccine , 10 days after infection, 3 C - group with intranasal administration of the vaccine, 30 days after infection. 1 B (s) - group with intramuscular administration of the vaccine, 5 days after infection, 2 B - group with intramuscular administration of the vaccine, 10 days after infection, 3 B - group with intramuscular injection of the vaccine, 30 days after infection.

4. Discussion

Scientists have conducted experiments over the past decades and have collected sporadic but convincing data on the possibility of using nucleic acids as an active immunogen [26, 27]. Still, there are two serious questions that should be addressed.

First, the question of whether dendritic cells can present an antigen fragment of an oligonucleotide vaccine containing a unique sequence of coronavirus RNA genomes remains insufficiently studied. Leukocytes and dendritic cells are able to penetrate into all parts of the body, since they have the qualities of absorption, transport, processing and presentation of antigens to T lymphocytes [28]. Dendritic cells move to secondary lymphoid organs to provide delivery of antigens to T lymphocytes and this, in turn, contributes to the manifestation of a powerful antigen-specific immune response. If B cells are affected when an antigen is detected, then this also applies to T cells, since B cells cannot be involved on alone in immune response [29]. This suggests that if B cells are activated, then so are T cells, whose full activation depends on dendritic cells. Currently, there is no single antigen that can activate B cells without activating T cells. However, in systemic lupus erythematosus, B cells are activated and antibodies are produced that attack the DNA of cells of a sick person [26, 27], but activation of T cells by dendritic cells due to antigen presentation of nucleic acid fragments has not yet been shown. To date, this issue has not yet been closely studied yet.

Second, we assume that the human body can contain antibodies that can enter human cells during viral infection and target particular fragments of nucleic acids in RNA viruses. While generally speaking, antibodies do not pass easily through intact cellular or subcellular membranes in

living cells [30], obviously that this is not always the case. Numerous investigations conducted mostly in cultured cells over the years have demonstrated that it is possible to facilitate the cellular internalization of antibodies [31]. The potential for in vivo therapeutic advantages of a nuclear-penetrating lupus anti-DNA autoantibody have also been shown in a number of studies [32, 33]. Thus, the ability of oligonucleotide vaccines will be determined by the ability of dendritic cells to make antigen presentation of coronavirus oligonucleotide sequences, as well as the ability of antibodies to attack unique coronavirus sequences inside infected host cells.

5. Conclusions

This manuscript for the first time offers for consideration the results of studies with the constructions of an oligonucleotide vaccine of the La-S-so type. The data obtained indicate a positive effect of the La-S-so type oligonucleotide vaccine on the weight of transgenic mice, as well as on the organometric parameters and cellular structure of the lung tissue. The observed effects, in our opinion, cannot be explained only by the presence of an inline adjuvant (CpG islands) in the vaccine design, although they undoubtedly make a significant contribution to the observed effects.

In the absence of developed test systems capable of assessing the formation of antibodies to the administered oligonucleotide vaccine, the data obtained indirectly indicate the prospects for the development of this vaccine platform. The synthesis of oligonucleotide vaccines can be automated relatively easily and prepare us for the next encounter with the SARS-CoV-2 coronavirus pandemic, unfortunately, there is no doubt that it will happen again. Further research will be aimed at proving 1) the existence antibodies capable of penetrating cells and attacking the unique nucleic acid sequences of RNA viruses, and 2) antigen presentation ability of dendritic cells with respect to nucleic acids. In our opinion, even oligonucleotide vaccines do not yet fit within the framework of a modern textbook on immunology, they have a great potential in prophylaxis of COVID-19 and other diseases caused by coronaviruses.

Author Contributions: Conceptualization, V.V.O.; methodology, V.V.O., K.A.Y., and T.P.M; software, I.A.N.; formal analysis, V.V.O. and K.V.L.; investigation, V.V.O., K.A.Y., and T.P.M.; resources, I.A.N., A.V.K; data curation, V.V.O. and K.V.L.; writing—original draft preparation, V.V.O.; writing—review and editing, V.V.O., K.A.Y., O.A.A., and A.I.B.; visualization, V.V.O. and K.A.Y.; supervision, V.V.O.; project administration, V.V.O. and K.V.L. All authors have read and agreed to the published version of the manuscript.

Funding: The research results are obtained within the framework of as state assignment V.I. Vernadsky Crimean Federal University for 2021 and the planning period of 2022–2023 No. FZEG-2021-0009 ('Development of oligonucleotide constructs for making selective and highly effective preparations for medicine and agriculture', registration number 121102900145-0).

Conflicts of Interest: The authors declare no conflict of interest.

References

1. Johns Hopkins Coronavirus Resource Center. Available online: https://coronavirus.jhu.edu/map.html (accessed on 10 March 2023).
2. Is the worst of the pandemic over for Europe? *Lancet Regional Health—Europe* **2021**, 2,100077. doi:10.1016/j.lanepe.2021.100077.
3. Ai, J.; Zhang, H.; Zhang, Y.; Lin, K.; Zhang, Y.; Wu, J.; Wan, Y.; Huang, Y.; Song, J.; Zhangfan, F. et al. Omicron variant showed lower neutralizing sensitivity than other SARS-CoV-2 variants to immune sera elicited by vaccines after boost. *Emerg. Microbes Infect.* **2022**; *1*, 337–343. doi:10.1080/22221751.2021.2022440.
4. Eliakim-Raz, N.; Stemmer, A.; Ghantous, N.; Ness, A.; Awwad, M.; Leibovici-Weisman, Y.; Stemmer, S.M. Antibody Titers After a Third and Fourth SARS-CoV-2 BNT162b2 Vaccine Dose in Older Adults. *JAMA Netw. Open* **2022**; *5*, e2223090. doi: 10.1001/jamanetworkopen.2022.23090.
5. Del Rio, C.; Malani, P.N. COVID-19 in 2022-The Beginning of the End or the End of the Beginning? *JAMA* **2022**, *327*, 2389-2390. doi: 10.1001/jama.2022.9655.
6. Agrawal, A.S.; Tao, X.; Algaissi, A.; Garron, T.; Narayanan, K.; Peng, B.H.; Couch, R.B.; Tseng, C.T. Immunization with inactivated Middle East Respiratory Syndrome coronavirus vaccine leads to lung immunopathology on challenge with live virus. *Hum. Vacci.n Immunother.* **2016**, *0*, 1-6. doi: 10.1080/21645515.2016.1177688.

7. Voysey, M.; Clemens, S.A.C.; Madhi, S.A.; Weckx, L.Y.; Folegatti, P.M.; Aley, P.K.; Angus, B.; Baillie, V.L..; Barnabas, S.L.; Bhorat, Q.E.; et al. Safety and efficacy of the ChAdOx1 nCoV-19 vaccine (AZD1222) against SARS-CoV-2: an interim analysis of four randomised controlled trials in Brazil, South Africa, and the UK. *Lancet* **2021**, 1-13. doi: 10.1016/S0140-6736(20)32661-1.
8. Sekar, A.; Campbell, R.; Tabbara, J.; Rastogi, P. ANCA glomerulonephritis after the Moderna COVID-19 vaccination. *Kidney Int*. **2021**, *100*, 473-474. doi: 10.1016/j.kint.2021.05.017.
9. Mallapaty, S. China COVID vaccine reports mixed results—what does that mean for the pandemic? *Nature* **2021**. doi: 10.1038/d41586-021-00094-z.
10. Gras-Champel, V.; Liabeuf, S.; Baud, M.; Albucher, J.F.; Benkebil, M.; Boulay, C.; Bron, A.; El Kaddissi, A.; Gautier, S.; Geeraerts, T. et al. Atypical thrombosis associated with VaxZevria® (AstraZeneca) vaccine: data from the French Network of Regional Pharmacovigilance Centres. *Therapies* **2021**, *76*, 369-373. doi: 10.1016/j.therap.2021.05.007.
11. European Medicines Agency. Available online: https://www.ema.europa.eu/en/documents/assessment-report/covid-19-vaccine-astrazeneca-epar-public-assessment-report_en.pdf (accessed on 29 January 2021).
12. Lee, L.A.; Franzel, L.; Atwell, J.; Datta, S.D.; Friberg, I.K.; Goldie, S.J.; Reef, S.E.; Schwalbe, N.; Simons, E.; Strebel, P.M.; Sweet, S.; Suraratdecha, C.; Tam, Y.; Vynnycky, E.; Walker, N.; Walker, D.G.; Hansen, P.M. The estimated mortality impact of vaccinations forecast to be administered during 2011–2020 in 73 countries supported by the GAVI Alliance. *Vaccine* **2013**, *31*, B61–B72. doi:10.1016/j.vaccine.2012.11.035.
13. Oberemok, V.V.; Andreeva, O.A.; Laikova, K.V.; Novikov, I.A.; Kubyshkin, A.V. Post-genomic platform for development of oligonucleotide vaccines against RNA viruses: diamond cuts diamond. *Inflamm. Res*. **2022**, *71*, 729–739. doi: 10.1007/s00011-022-01582-2.
14. Lai, C.Y.; Yu, G.Y.; Luo, Y.; Xiang, R.; Chuang, T.H. Immunostimulatory Activities of CpG-Oligodeoxynucleotides in Teleosts: Toll-Like Receptors 9 and 21. *Front. Immunol*. **2019**, *10*. doi: 10.3389/fimmu.2019.00179.
15. Thompson, J.D.; Higgins, D.G.; Gibson, T.J. CLUSTAL W: improving the sensitivity of progressive multiple sequence alignment through sequence weighting, position-specific gap penalties and weight matrix choice. *Nucleic Acids Res.* **1994**, *22*, 4673–4680. doi:10.1093/nar/22.22.4673.
16. Krieg, A.M.; Wagner, H. Causing a commotion in the blood: immunotherapy progresses from bacteria to bacterial DNA. *Immunol. Today* **2000**; *21*:521–6. doi:10.1016/S0167-5699(00)01719-9.
17. Oberemok, V.V.; Laikova, K.V.; Yurchenko, K.A.; Marochkin, N.A.; Fomochkina, I.I.; Kubyshkin, A.V. SARS-CoV-2 will constantly sweep its tracks: a vaccine containing CpG motifs in 'lasso' for the multi-faced virus. *Inflamm. Res.* **2020**, *69*, 801–812. doi:10.1007/s00011-020-01377-3
18. Haas, T.; Metzger, J.; Schmitz, F.; Heit, A.; Müller, T.; Latz, E.; Wagner, H. The DNA sugar backbone 2′ deoxyribose determines toll-like receptor 9 activation. *Immunity* **2008**, *28*, 315–23. doi: 10.1016/j.immuni.2008.01.013.
19. Ballas, Z.K.; Rasmussen, W.L.; Krieg, A.M. Induction of NK activity in murine and human cells by CpG motifs in oligodeoxynucleotidesand bacterial DNA. *J Immunol*. **1996**, *157*, 1840–5. PMID: 8757300.
20. Yamamoto, S.; Yamamoto, T.; Kataoka, T.; Kuramoto, E.; Yano, O.; Tokunaga, T. Unique palindromic sequences in synthetic oligonucleotides are required to induce IFN [correction of INF] and augment IFN-mediated [correction of INF] natural killer activity. *J. Immunol*. **1992**, *148*, 4072–6. PMID: 1376349.
21. Electronic scientific and practical research journal "Modern scientific and innovation" Available online: https://web.snauka.ru/issues/2016/07/69677 (accessed on 7 April 2023).
22. Kumar, D.; Bayry, J.; Hegde, N.R. COVID-19: A Veterinary and One Health Perspective. *J. Indian Inst. Sci.* **2022**, *102*, 689-709. doi: 10.1007/s41745-022-00318-9.
23. Bouvier, N.M.; Lowen, A.C. Animal models for influenza virus pathogenesis and transmission. *Viruses* **2010**, *2*, 1530–1563. doi: 10.3390/v20801530
24. Thangavel, R.R.; Bouvier, N.M. 2014. Animal models for influenza virus pathogenesis, transmission, and immunology. J. *Immunol. Methods* **2014**, *410*, 60–79. doi: 10.1016/j.jim.2014.03.023.
25. Felgenhauer, J.L.; Brune, J.E.; Long, M.E.; Manicone, A.M.; Chang, M.Y.; Brabb, T.L.; Altemeier, W.A.; Frevert, C.W. Evaluation of Nutritional Gel Supplementation in C57BL/6J Mice Infected with Mouse-Adapted Influenza A/PR/8/34 Virus. *Comp. Med.* **2020**, *70*, 471-486. doi: 10.30802/AALAS-CM-20-990138.
26. Pisetsky, D.S.; Reich, C.F. The binding of anti-DNA antibodies to phosphorothioate oligonucleotides in a solid phase immunoassay. *Mol. Immunol.* **1998**, *35*, 1161–70. doi: 10.1016/s0161-5890(98)00108-4.
27. Pisetsky, D.; Vrabie, I. Antibodies to DNA: infection or genetics? *Lupus* **2009**, *18*, 1176-1180. doi:10.1177/0961203309106492.
28. Dieli, F. Dendritic cells and the handling of antigen. *Clin. Exp. Immunol.* **2003**, *134*, 178–80. doi:10.1046/j.1365-2249.2003.02279.x.
29. Langelaar, J.; Rijvers, L.; Smolders J.; Luijn, M.M. B and T cells driving multiple sclerosis: identity, mechanisms and potential triggers. *Front Immunol.* **2020**, *11*. doi:10.3389/fimmu.2020.00760.
30. Muller, S.; Zhao, Y.; Brown, T.L.; Morgan, Al.C.; Kohler, H. TransMabs: cell-penetrating antibodies, the next generation. *Expert Opin. Biological. Ther*. **2005**, *5*, 237–41. doi:10.1517/14712598.5.2.237.

31. Lackey, C.A.; Press, O.W.; Hoffman, A.S.; Stayton, P.S. A biomimetic pH-responsive polymer directs endosomal release and intracellular delivery of an endocytosed antibody complex. *Bioconjug. Chem.* **2002**, *13*, 996–1001. doi: 10.1021/bc010053l.
32. Noble, P.W.; Young, M.R.; Bernatsky, S.; Weisbart, R.H.; Hansen, J.E. A nucleolytic lupus autoantibody is toxic to BRCA2-deficient cancer cells. *Sci. Rep*. **2014**, *4*. doi: 10.1038/srep05958.
33. Weisbart, R.H.; Chan, G., Jordaan, G.; Noble, P.W.; Liu, Y.; Glazer, P.M.; Nishimura, R.N.; Hansen, J.E. DNA-dependent targeting of cell nuclei by a lupus autoantibody. *Sci. Rep.* **2015**, *5*. doi: 10.1038/srep12022.